

***Stardust* cometary and interstellar dust collector calibration: modelling impacts on Al-1100 foil at velocities up to 20 km s⁻¹ and comparison with experimental data.**

M. C. Price (1), A. T. Kearsley (2) and M. J. Burchell (1)

(1) Centre for Astrophysics and Planetary Science, University of Kent, Canterbury, CT2 7NH, UK
mcp2@star.kent.ac.uk.

(2) IARC, Dept. of Mineralogy, The Natural History Museum, London, SW7 5BD, UK.

Abstract

We demonstrate cometary and interstellar dust size calibration using computer simulations of impacts on the foil sections of the collector on NASA's *Stardust* [1] mission. We have used the *Ansys Autodyn* [2] software package to model impacts into Stardust foil (100 μm thick Al-1100) at velocities from 1 – 20 km s⁻¹ with silica and soda-lime glass projectiles with diameters between 500 nm – 22 μm . Experimental data from light gas gun (LGG) shots of projectiles with tightly constrained size are compared with modelling results to create multiple validation tie-points for impacts by small particles at the Wild 2 cometary dust encounter velocity of 6.1 km s⁻¹. Following experimental validation for a range of velocities from 1 to 7.5 km s⁻¹, the numerical model is then used to extrapolate to crater dimensions expected from higher velocity impacts by interstellar dust grains with diameters of 2 and 20 μm .

Modelling details

A Cowper-Symonds [3] strength model and a Mie-Gruneisen equation-of-state were used as material parameters for the Al-1100 target. This strength model enables the modelling of the effects of the very high strain rates ($>>10^8 \text{ s}^{-1}$) present during the impact. A 2-D 300 (y) x 200 (x) cell half-space Lagrangian mesh was used to model the target. The mesh was graded so as to give a high resolution (cell size = 0.05 x projectile radius) at the impact region. Shock transmission boundaries were placed on the edges of the target to emulate a semi-infinite target.

Experimental methodology

Shots were performed using the Kent two-stage LGG [4]. The projectiles were monodisperse silica (for projectiles with diameter < 10 μm) and

soda-lime glass spheres (diameters > 10 μm) commercially available from Micromod (Germany) and Whitehouse Scientific (UK) respectively. SEM/EDX imaging of projectiles and impacted foil targets was carried out at the Natural History Museum using a carefully calibrated JEOL 5900 LV SEM. Craters were measured following the method of [5]; crater diameters, D_C , were defined as the distance from top of the crater lip to the top of the diametrically opposed crater lip.

Comparison with experimental data (6 km s⁻¹)

Numerous experimental data from earlier work [6] are available for comparison to modelling of larger craters (> 40 μm diameter). However, most Stardust cometary craters are much smaller [7], prompting us to perform a new suite of calibration experiments [8]. Our projectiles now also overlap the size range appropriate for calibration of interstellar dust impacts on Stardust, although we cannot achieve the high velocity range [9] by LGG.

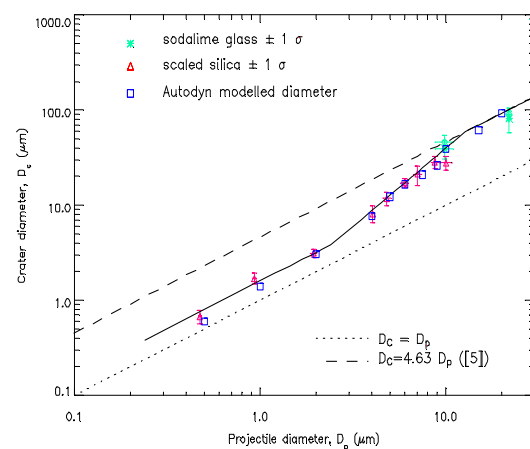


Figure 1: *Autodyn* modelled data vs. experimental data for impacts at a velocity of 6.1 km sec⁻¹, note good agreement between experiment and model.

To take into account the density difference between the two projectile materials ($\rho_{\text{silica}} = 2.2 \text{ g cm}^{-3}$, $\rho_{\text{sodalime}} = 2.4 \text{ g cm}^{-3}$), silica crater diameters were increased by 4%, according to the formula of [6]. *Autodyn* model output is in very good agreement with the experimental data. In particular the change of the projectile and crater size relationship seen to occur in shots of grains between 2 and 10 μm is well reproduced, we attribute this to a function of the higher strain rates produced by impact of smaller projectiles.

Impact speeds above 6.1 km sec^{-1}

Sawle [9] detailed experiments with Pyrex spheres accelerated using a plasma rail-gun to a velocity of approximately 15 km s^{-1} and then impacted onto Al-1100 and Al-2014 T6 foils and semi-infinite targets. The results for impacts on semi-infinite Al-1100 are summarised in Table 1. Also given are the results from our *Autodyn* simulations (using the same parameters as above) for glass spheres within the diameter range as [9]. The last column in Table 1 gives the crater depth.

Table 1: Experimental and modelled crater dimensions for a 125 μm diameter Pyrex projectile impacting an Al-1100 target at 15 km s^{-1} .

	V (km sec^{-1})	D_p (μm)	D_C (μm)	Depth (μm)
Sawle [9]	15 ± 0.75	127 ± 25	965 ± 48	474 ± 28
Autodyn	15.00	125.00	1023.00	491.00

Autodyn output for a modelled 125 μm diameter glass projectile falls close to experimental data of [9], within 5% (although just outside stated errors), giving us confidence in the accuracy of the Al-1100 strength model at high speeds.

We next modelled the crater diameter expected for 2 μm and 20 μm glass projectiles as a function of impact velocity (Fig. 2). The larger projectiles show that crater size is controlled by velocity over the whole range, albeit with different behaviour above and below 6 km s^{-1} . Smaller projectiles, however, do not show a substantial change in crater diameter. More modelling is needed to establish if the difference in behaviour is again due to strain rate effects.

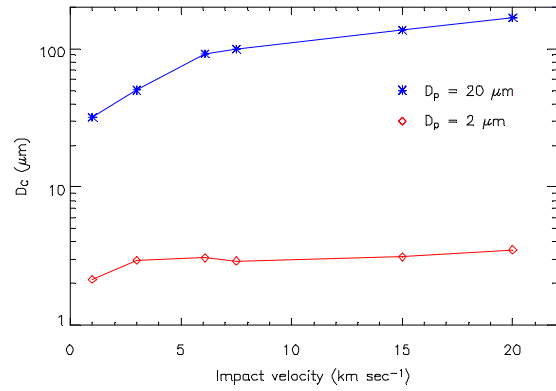


Figure 2: Modelled crater diameter versus impact velocity for 2 μm and 20 μm diameter projectiles

Conclusions

We can now present a model for craters on the interstellar collection foils of *Stardust*. The model has been optimised to work for micron scale projectiles and over a wide speed range (up to 20 km s^{-1}). We find that the model accurately predicts the crater diameter for projectile diameters of 500 nm – 30 μm at 6.1 km s^{-1} . For particles smaller than 2 μm , the crater diameter is virtually constant for impact velocities between 3 - 20 km s^{-1} . Large projectiles show a dependence of crater size on impact speed, which differs above and below 6 km s^{-1} . We hope soon to be able to compare our models with results obtained experimentally from high speed shots at the Heidelberg dust accelerator.

References

- [1] Brownlee D. E. et al. (2006), *Science*, 314, 1711–1716.
- [2] ANSYS Inc., <http://www.ansys.com/> (accessed May 2009).
- [3] Cowper G. R. & Symonds P. S. (1957), *Tech. Report*, #28, Brown University.
- [4] Burchell M. J. et al. (1999), *Meas. Sci. Tech.*, 10, 41–50.
- [5] Kearsley A. T. et al. (2006), *MAPS.*, 41, 167–180.
- [6] Kearsley A.T. et al. (2007) *MAPS.*, 42, 191–210.
- [7] Hörlz F. et al. (2006) *Science*, 314, 1716-1719.
- [8] Price M. C. et al. (2009), *LPSC XXXX*, Abstract #1564.
- [9] Sawle, D. R. (1970), *AIAA Journal*, Vol. 8, No. 7, 1240 – 1244.